Molecular Vision 2014; 20:670-682 <http://www.molvis.org/molvis/v20/670>
Received 8 December 2013 | Accepted 24 May 2014 | Published 27 May 2014

Gap junction proteins in the light-damaged albino rat

Cindy X. Guo,[1,3] Henry Tran,[1] Colin R. Green,[2,3] Helen V. Danesh-Meyer,[2,3] Monica L. Acosta[1,3]

[1]Department of Optometry and Vision Science, University of Auckland, Auckland, New Zealand; [2]Department of Ophthalmology, University of Auckland, Auckland, New Zealand; [3]New Zealand National Eye Centre, University of Auckland, Auckland, New Zealand

Purpose: Changes in connexin expression are associated with many pathological conditions seen in animal models and in humans. We hypothesized that gap junctions are important mediators in tissue dysfunction and injury processes in the retina, and therefore, we investigated the pattern of connexin protein expression in the light-damaged albino rat eye.
Methods: Adult Sprague-Dawley rats were exposed to intense light for 24 h. The animals were euthanized, and ocular tissue was harvested at 0 h, 6 h, 24 h, 48 h, and 7 days after light damage. The tissues were processed for immunohistochemistry and western blotting to analyze the expression of the gap junction proteins in the light-damaged condition compared to the non-light-damaged condition. Cell death was detected using the terminal deoxynucleotidyl transferase-mediated dUTP nick-end labeling (TUNEL) technique.
Results: Intense light exposure caused increased TUNEL labeling of photoreceptor cells. Immunocytochemistry revealed that connexin 36 (Cx36) was significantly increased in the inner plexiform layer and Cx45 was significantly decreased in the light-damaged retina. The pattern of Cx36 and Cx45 labeling returned to normal 7 days after light damage. Cx43 significantly increased in the RPE and the choroid in the light-damaged tissue, and decreased but not significantly in the retina. This elevated Cx43 expression in the choroid colocalized with markers of nitration-related oxidative stress (nitrotyrosine) and inflammation (CD45 and ionized calcium-binding adaptor molecule-1) in the choroid.
Conclusions: The results suggest that connexins are regulated differently in the retina than in the choroid in response to photoreceptor damage. Changes in connexins, including Cx36, Cx43, and Cx45, may contribute to the damage process. Specifically, Cx43 was associated with inflammatory damage. Therefore, connexins may be candidate targets for treatment for ameliorating disease progression.

Gap junction channels, formed by the docking of two hemichannels, allow for the rapid exchange of ions, messengers, and metabolic molecules between neighboring cells [1]. Each hemichannel is formed by the oligomerization of six connexin proteins [2]. Intercellular communication is involved in a wide range of cellular activities, including cell signaling, differentiation, and growth [3]. In addition to direct intercellular channel communication, many studies suggest that non-junctional hemichannels may release signaling molecules into the extracellular space or allow Ca^{2+} wave propagation [4-6]. In the retina, gap junctions are expressed in five major types of neurons and participate in electrical coupling between cells for light sensation [7]. Connexin 36 (Cx36; OMIM 607058) and Cx45 (OMIM 608655) are predominantly expressed in the inner plexiform layer of the retina [8] and have been identified as key elements in the light signal transduction pathways [7]. Cx43 is the most ubiquitous gap junction protein, however, and is expressed by astrocytes and the endothelium. Previous studies have demonstrated that Cx43 (OMIM 121014) plays a role in Müller cells, astrocytes, the vascular endothelium, and the RPE in human and rat retinas [8,9].

Gap junctions may contribute to the passage of molecules including death signals from a stressed cell to its surrounding cells. This can be a damaging process that spreads stress or injury signals as well as a protective process that buffers toxic substances [10]. Reports have suggested that changes in gap junctions occur under several pathological conditions and diseases such as Cx32 (OMIM 304040) mutation in X-linked Charcot-Marie-Tooth disease, Cx50 (OMIM 600897) and Cx46 (OMIM 121015) mutations in zonular pulverulent cataract, and Cx26 (OMIM 121011) mutations in hereditary non-syndromic sensorineural deafness [11]. In retinitis pigmentosa, rod-specific proteins, such as rhodopsin, are genetically affected, and gap junctions have been suggested to perform the "bystander effect" of passing cell death signals or endogenous agents from dying rods to genetically normal cones [12]. Furthermore, increased Cx43 expression has been reported in ischemic and diabetic animal models [13,14], glaucoma [15], and central nervous system diseases [16-18]. We hypothesized that gap junctions contribute to tissue dysfunction and injury processes. We used light-damaged albino rats as an animal model to investigate changes in gap junction expression during the complex series of events following light

Correspondence to: Monica Acosta, Department of Optometry and Vision Science, The University of Auckland. Private Bag 92019, Auckland, New Zealand; Phone: +64 9 9236069; FAX: +64 9 373 7485; email: m.acosta@auckland.ac.nz

damage that may comprise oxidative stress, inflammation, and vascular reactions. The aim was to identify possible connexin roles in retinal disease such as age-related macular degeneration.

The albino rat exposed to intense fluorescent light has been an animal model of retinal degeneration since the 1960s [19]. Retinal function is significantly affected following light damage as shown by dramatically dropped a- and b-waveforms in electroretinogram (ERG) tests [19]. Histological analysis of the light-damaged animal model has shown changes in Müller cells, loss of photoreceptors and pigment epithelium, breakage of Bruch's membrane, and choroidal damage [19-21]. The mechanisms of retinal degeneration in the animal model induced by light damage, however, remain unclear. Oxidative stress in photoreceptors results from the process of photo-oxidation generated by rhodopsin bleaching in photoreceptor outer segments and is observed in the RPE as a result of phagocytosis of the outer segment [22]. The retinal stress initiated by excessive rhodopsin bleaching consequently spreads into the RPE and choriocapillaris [22]. Inflammation is involved in the pathogenesis of age-related macular degeneration (AMD) [23, 24] and has been found in the light-damaged animal model [25,26]. Although the adult retina is regarded as an immune-privileged tissue, the retina has residential glial cells that provide support to and protect the retinal neurons by supplying nutrients, removing neural waste products, and phagocytozing neuronal debris [27]. Retinal microglia become activated after light damage and migrate to the outer retina in several animal models [25,26]. An inflammatory response is present in the retina and the choroid following light damage [25], suggesting residential microglia and macrophage activation, and migration may play an important role in the process of tissue damage in the light-damaged albino animal model.

Based upon previous studies, we hypothesized that retinal stress may be initiated by excessive bleaching of rhodopsin in the photoreceptors that results from prolonged exposure to the intense light. This would consequently result in disruption of the outer retinal blood barrier, mainly the RPE. This injury involves processes of abnormal cation influx, oxidative damage, and activation of an inflammatory response that would lead to secondary injury of the retinal neurons and result in retinal degeneration [25,26,28]. Oxidative damage and its associated inflammatory response are sufficient to produce lesions in the retina and the choroid [29]. Alterations in gap junctions expressed on retinal neurons together with photoreceptor degeneration may contribute to photoreceptor and post-photoreceptor dysfunction in the retina in the animal model. Similar to other animal injury models [13,14,30], Cx43 expression may be affected after intense light-induced injury. The present study was to evaluate changes in the expression of connexin proteins, especially Cx43, in the light-damaged rat retina and to evaluate changes in neuronal function, oxidative stress, inflammatory response, and vascular reactions.

METHODS

Animals: All experimental procedures described in this study were approved by the University of Auckland Animal Ethics Committee and comply with the use of animals in eye research. Adult Sprague-Dawley (SD) rats (200–250 g, male or female) were used in this study. The SD rat is an albino strain and ensures the precise and direct effect of light on photoreceptor degeneration [19,20]. Animals were sourced from the Vernon Jansen Unit at the University of Auckland. Light in the animal breeding unit was provided by white fluorescence light (Philips Master TLD 18W/965; Koninklijke Philips Electronics N.V., Shanghai, China). The light source covers broad band fluorescence, from 380 to 760 nm, and the average intensity at the top of the cage is 120 W/m^2. The animals used in these experiments were housed in normal cyclic light conditions [12 h light (174 lux):12 h dark (<62 lux)] for the duration of the study, except where otherwise stated.

Light damage procedure: Intense light was used to damage the retina in albino rats. Light damage experiments started consistently around 9:00 AM. The luminance was 2,700 lux, created by placing fluorescent light lamps (Philips Master TLD 18W/965) directly above the rat cages. The light source covered broad band fluorescence, from 380 to 760 nm, with no heat generated by the light source. This broad band fluorescence light has been used in a previous study [28]. Continuous exposure was achieved by removing hiding places in the cages. Animals were able to move freely in the cage and had free access to food and water. Non-light-damaged animals were used in the control group. All experimental protocols consisted of 24 h light exposure with variable recovery periods (0 h, 6 h, 24 h, 48 h, or 7 days) in normal 12 h light (174 lux):12 h dark (<62 lux) conditions.

Tissue collection: The animals were deeply anesthetized with intraperitoneal injection (i.p.) with a combination of ketamine (75 mg/kg) and domitor (0.5 mg/kg). The rat's chest cavity was opened, and a perfusion needle was inserted into the left ventricle. An outlet was made in the right atrium to enable the flush solution and fixative to circulate through the vasculature. The animals were perfused with saline for 2–3 min. For the tissue collected for immunohistochemical procedures, the animals were further perfused with 4% paraformaldehyde (PFA) in a 0.1 M phosphate buffer (PB) for 2–3 min. After transcardial perfusion, the eyes were dissected

from the orbit. The posterior eyecup was flattened by making several radial cuts in the margin. A strip of the central retina across the temporal/nasal axis 1 mm above the optic nerve was dissected. In an intense light damage paradigm, the dorsal arc of the retina is affected the most; the molecular and morphological reasons were reviewed by Organisciak and Vaughan [31]. In this study, the central part of the dorsal retina was used. With the sclera side up, the tissue was gently mounted on filter paper (0.8 µm pore size, Gelman Sciences, Ann Arbor, MI) to keep the tissue flat for cryosectioning. The tissue was then further fixed in 4% PFA for 30 min at room temperature and washed in 0.1 M PBS (1X; 154 mM NaCl, 72 mM Na_2HPO_4, 19 mM NaH_2PO_4, pH 7.4). The tissue was cryoprotected using graded sucrose solutions 10% and 20% for 30 min each at room temperature and 30% overnight at 4 °C, and frozen in Tissue-Tek optimum cutting temperature (OCT) compound (Sakura Finetek, Torrance, CA) at −20 °C. The tissue was then cryosectioned in the vertical plane of the retina (16 µm sections) using a cryostat (Leica CM3050S, Heidelberg, Germany). The sections were collected on SuperFrost Plus slides (Labserv, Auckland, New Zealand) and stored at −20 °C until the start of immunolabeling or the staining procedures.

Terminal deoxynucleotidyl transferase-mediated dUTP nick-end labeling staining (TUNEL) and cell death analysis: Cell death was investigated in light-damaged and non-light-damaged retina. The TUNEL technique was used to detect cell death. Tissues were processed using a commercial In Situ Cell Death Detection Kit, Fluorescein (Roche Applied Science, Mannheim, Germany). Tissue sections were washed twice with 0.1 M PBS before being permeabilized with 0.1% Triton X-100 and 0.1% trisodium citrate in 0.1 M PBS for 5 min on ice. The sections were washed and incubated with the TUNEL reaction mixture (TdT enzyme solution and fluorescein nucleotide label solution at 1:17 dilution) for 20 min at 37 °C in a dark humid chamber. Negative controls were incubated with the label solution only. The sections were rinsed several times in 0.1 M PBS, and then mounted in Vectashield HardSet Mounting Medium with 4',6-diamidino-2-phenylindole dihydrochloride (DAPI; Vector Laboratories, Burlingame, CA). The stained sections were visualized using confocal microscopy.

Immunohistochemistry: Frozen tissue sections were air-dried at room temperature for 10 min and then washed in 0.1 M PBS. The tissue sections were encircled with a PAP pen (Life Technologies, Camarillo, CA) after the excess moisture around the sections was wiped off. Non-specific binding sites in the tissue were blocked with 6% normal goat serum (NDS from Sigma-Aldrich, Saint Louis, MO) or normal donkey serum (NGS from Invitrogen, Frederick, MD), 1% bovine serum albumin (BSA), and 0.5% Triton X-100 in 0.1 M PBS for 1 h at room temperature. The primary antibodies were diluted in antibody solution containing 3% normal goat serum or normal donkey serum, 1% BSA, and 0.5% Triton X-100 in 0.1 M PBS (primary antibody details; Table 1) and were applied carefully to cover the tissue sections. Tissue sections were incubated with the primary antibody overnight at room temperature. The negative control for each antibody was conducted by incubating sections with antibody solution only following the same protocol as if a primary antibody was applied. After the overnight incubation, the slides were washed three times for 5 min each in 0.1 M PBS and once for 15 min in 0.1 M PBS to remove excess primary antibodies. The secondary antibodies, goat anti-rabbit, goat anti-mouse, or donkey anti-guinea pig, conjugated to either Alexa 488 or Alexa 594 (Life Technologies, Carlsbad, CA), were diluted 1:500 in antibody solution and applied to the tissue for 2 h at room temperature. Slides were washed thoroughly with 0.1 M PBS to remove all excess secondary antibodies. Following the washes, the tissue sections were incubated with DAPI (Sigma) 1 µg/ml in 0.1 M PBS for 15 min to label cell nuclei, followed by another thorough wash with 0.1 M PBS. The slides were then mounted in a non-fluorescence-fading medium (Citifluor, London, UK) and sealed with nail polish to avoid leakage and evaporation.

Imaging and fluorescence quantification: All the images correspond to the superior central retina area. The images were acquired using a high-resolution laser scanning confocal microscope (Olympus FluoView FV1000, Olympus Corporation, Tokyo, Japan) with 405, 473, and/or 559 nm excitation from an argon ion laser. A series of four to eight optical sections with 1 µm interval were collected for each specimen, and image analysis was performed on an image stack intensity projection over the z-axis. All images were acquired with the same gain and brightness. Six retinas obtained from different animals were analyzed for each group, and the representative image for each condition is shown.

Fluorescence quantification was performed using ImageJ 1.45s software (Wayne Rasband, National Institutes of Health, Bethesda, MD). RGB images were converted to binary mode. The background was set on a non-labeled area of the slide. The number of pixels occupied by the marker was measured in a constant 200 µm × 150 µm area of the central-superior retina in at least eight regions per tissue section (n = 6).

Western blotting: The tissues used in the western blot procedure were processed immediately after the animals were deeply anesthetized with a combination of ketamine (75 mg/kg) and domitor (0.5 mg/kg). After transcardial perfusion and

Table 1. List of primary antibodies used in this study.

Antibody	Production	Host	Working dilution	Company	Cat No.	Immunogen	Reference
Anti-Cx43	Polyclonal	Rb	1:1000	Sigma-Aldrich,	C6219	Synthetic peptide corresponding to amino acids 363–382 of human and rat Cx43	[9]
Anti-Cx36	Polyclonal	Rb	1:400	Life Technologies,	51–6300	Peptide corresponding to a sequence from the C-terminus of rat and mouse Cx36	[54]
Anti-Cx45	Polyclonal	Rb	1:100	Life Technologies,	40–7000	Synthetic peptide derived from the C-terminal region of the mouse, rat, Chinese hamster, and golden hamster Cx45	[55]
Anti-CD45	Monoclonal, clone OX-1	Ms	1:20	BD PharMingen	550,566	CD45-enriched glycoprotein fraction from Wistar rat thymocytes	[56]
Anti-nitrotyrosine	Monoclonal, clone 1A6	Ms	1:2000	Millipore Corporation, MA	05–233	Nitrated KLH (Keyhole Limpet Hemocyanin)	[57,58]
Anti-Iba1	Polyclonal	Gt	1:250	Abcam	Ab5076	Synthetic peptide corresponding to amino acids 135–147 of human Iba1	[59,60]

dissection of the eye from the orbit, the posterior segment of the eye was isolated. The retina was carefully separated from the choroid and sclera with the use of a dissection microscope. The extracted whole retina tissue was homogenized in a cold, freshly prepared homogenization buffer (10 mM 4-(2-hydroxyethyl)-1-piperazineethanesulfonic acid/HEPES; 0.25 M sucrose in MilliQ water, pH 7.4) containing 1× protease inhibitor cocktail (Complete Mini Tablet; Roche Diagnostics, Manheim, Germany) using a Teflon homogenizer, according to a protocol for retinal tissue homogenization using a Teflon homogenizer and a 0.9% NaCl solution [32]. Homogenized samples were centrifuged twice at 5000 ×g for 2 min in an Eppendorf centrifuge (5415R; Eppendorf, Hamburg, Germany). The samples were then centrifuged twice (5000 ×g for 2 min at 4 °C) to sediment any unhomogenized tissue, and the supernatant was stored at −20 °C until used in the western blot analysis.

Protein samples were mixed with a loading buffer (10:1) containing 0.1% bromophenol blue, 20% v/v glycerol, and 2% sodium dodecyl sulfate (SDS). Typically, about 9 µg of retinal or choroidal sample protein in a total volume of 20 µl was gently loaded into the leading wells of a 10% Mini-PROTEAN TGX Precast Gel (Bio-Rad Laboratories, Auckland, New Zealand). Proteins were separated according to molecular weight under electrophoresis using a Mini-Protean Tetra Cell (Bio-Rad Laboratories) with an SDS gel running buffer (25 mM Tris base; 19 mM glycine; 0.1% SDS in MilliQ water), which applies a negative charge to each protein in proportion to its molecular weight. A Precision Plus Protein All Blue Standard (Bio-Rad Laboratories) containing proteins with known molecular weights ranging from 10 to 250 kDa was loaded alongside the protein samples in each gel. The separated proteins were transferred from the gel to a polyvinylidene difluoride (PVDF) membrane (Roche Diagnostics) using a semidry transfer system: Trans-Blot Turbo Transfer Starter System (Bio-Rad Laboratories) with a small amount of transfer buffer (25 mM Tris base; 190 mM glycine; 15% methanol in MilliQ water, pH 8.4).

The membrane containing separated and transferred protein samples was incubated with a blocking solution (5% non-fat milk powder; 2% v/v normal goat serum in Tris-buffered saline-tween (TBS-T), containing 20 mM Tris hydrochloride; 137 mM sodium chloride; 0.1% v/v Tween-20, pH 7.2) for 2 h at room temperature. This was followed by incubating the membrane with the primary antibody overnight at 4 °C. The primary antibody (anti-Cx43 antibody, 1:4,000 dilution) was diluted with an antibody solution containing 2% non-fat milk powder and 2% v/v normal goat serum in TBS-T. Following three washes each of 15 min and one wash for 40 min in TBS-T, the membrane was incubated with a horseradish peroxidase-conjugated secondary antibody (donkey anti-rabbit immunoglobulin G, 1:5,000; Amersham Biosciences, Buckinghamshire, UK) for 1 h at room temperature. The membrane was then washed with another series of TBS-T.

The immunoblot was detected using an ECL Plus Western Blot Detection Reagents Kit (Amersham Biosciences). The horseradish peroxidase-conjugated to the secondary antibody catalyzes oxidation of the Lumigen PS-3 Acridan substrate (Blot Detection Reagents Kit, Buckinghamshire, UK), and this reaction produces sustained, high-intensity

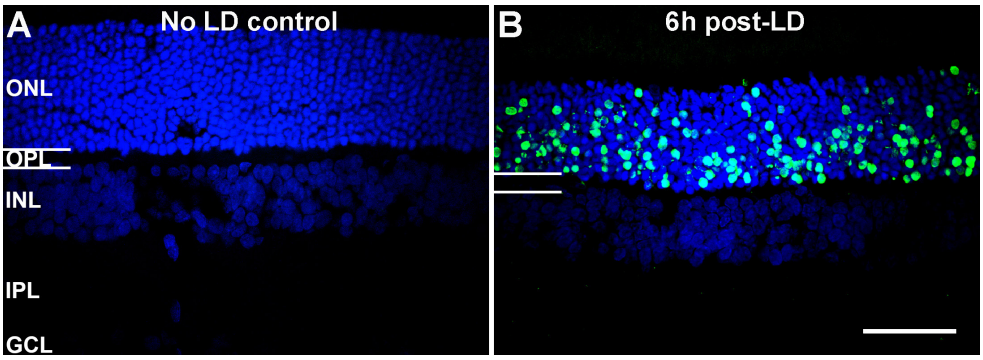

Figure 1. Terminal deoxynucleotidyl transferase-mediated uridine 5′-triphosphate-biotin nick end labeling (TUNEL) in the retina of the control and light-damaged rats. The images show 4',6-diamidino-2-phenylindole dihydrochloride (DAPI) labeling (blue) of the nuclei in the retina. In these images the ganglion cell layer (GCL) appears weakly labeled. **A**: Terminal deoxynucleotidyl transferase-mediated uridine 5′-triphosphate-biotin nick end labeling (TUNEL) labeling (green) was absent in the control rat in all retinal layers. **B**: TUNEL-positive cells were spread throughout the outer nuclear layer 6 h after light damage. At this time point no other retinal layers were TUNEL positive. Abbreviations: ONL, outer nuclear layer; INL, inner nuclear layer; OPL, outer plexiform layer; IPL, inner plexiform layer; GCL, ganglion cell layer. Scale bar = 50 µm.

chemiluminescence with maximum emission at a wavelength of 430 nm, which was subsequently detected on a FujiFilm LAS-4000 imager (GE Healthcare, Buckinghamshire, UK).

A loading control blot was performed following the imaging of the first immunoblot for anti-Cx43. The blot membrane was stripped out from the membrane by incubating it with stripping buffer (2% SDS, 100 mM β-mercaptoethanol, 62.5 mM Tris hydrochloride, pH 6.7) for 30 min at 37 °C. The loading control was then blotted with an anti-tubulin antibody (1:5,000 dilution in antibody solution) on the same membrane.

Quantification of the immunoblot images was conducted using ImageJ 1.45 s software (Wayne Rasband, National Institutes of Health). Histograms indicating the intensity of each band were obtained and converted into numerical values indicating the intensity of the bands with the ImageJ program. The blots for Cx43 were divided by the loading controls for each well, and then were statistically analyzed for the experimental groups.

Statistical analysis: Graphing and statistical analyses were performed using GraphPad Prism 6 (GraphPad Software, San Diego, CA). All data are presented as the mean±standard error of the mean (SEM). The comparison between normal and light-damaged tissue western blots for Cx43 was conducted using a one-way ANOVA followed by Tukey's test. Unpaired comparison was carried on using the Student *t* test with alpha = 0.05.

RESULTS

Photoreceptors were undergoing cell death in light damage: TUNEL labeling was performed on the central retinas in the normal control and light-damaged rats to provide an indication of the amount of photoreceptor cell loss (Figure 1). No TUNEL-positive cells were detected in the retinas of the control animals (Figure 1A). Six hours after light damage, there were a large number of TUNEL-positive cells in the outer nuclear layer, suggesting dramatic cell death and tissue damage (Figure 1B).

Expression of connexin 36 and connexin 45 is changed following light damage: The expression of Cx36 and Cx45 was investigated in the control and light-damaged animals using immunohistochemistry. In the control retinas, Cx36 immunoreactivity was low and limited to the inner plexiform layer and the RPE (Figure 2A). Labeling in the outer plexiform layer was not detectable. The high-magnification confocal image of the inner plexiform layer shows that punctate labeling was confined to the inner part of this layer (Figure 2E). At 24 h after light damage, immunoreactivity of Cx36 in the RPE was present but seemed to be redistributed within the cells. Small randomly distributed puncta labeling was seen in the outer plexiform layer. The Cx36 immunoreactivity in the inner plexiform layer appeared to increase (Figure 2B,F), and quantification indicated significant upregulation (Figure 2K; Student *t* test, $p<0.001$). At 7 days after light damage, Cx36 immunoreactivity in all layers was decreased to a level visually comparable to that of the control tissue (Figure 2G).

In the control retinas, Cx45 was mostly expressed in the inner plexiform layer distributed in a specific banding pattern. Labeling in the RPE and the outer segment of the photoreceptors was also evident (Figure 2C). In the nerve fiber layer, there was Cx45 expression possibly on vascular smooth muscle cells and astrocytes (Figure 2H, arrows). At 24 h after light damage, there was no evident change of Cx45 labeling in the RPE and outer segment area or in the nerve fiber layer, but interestingly, Cx45 immunoreactivity in the inner plexiform layer was decreased (Figure 2D,I).

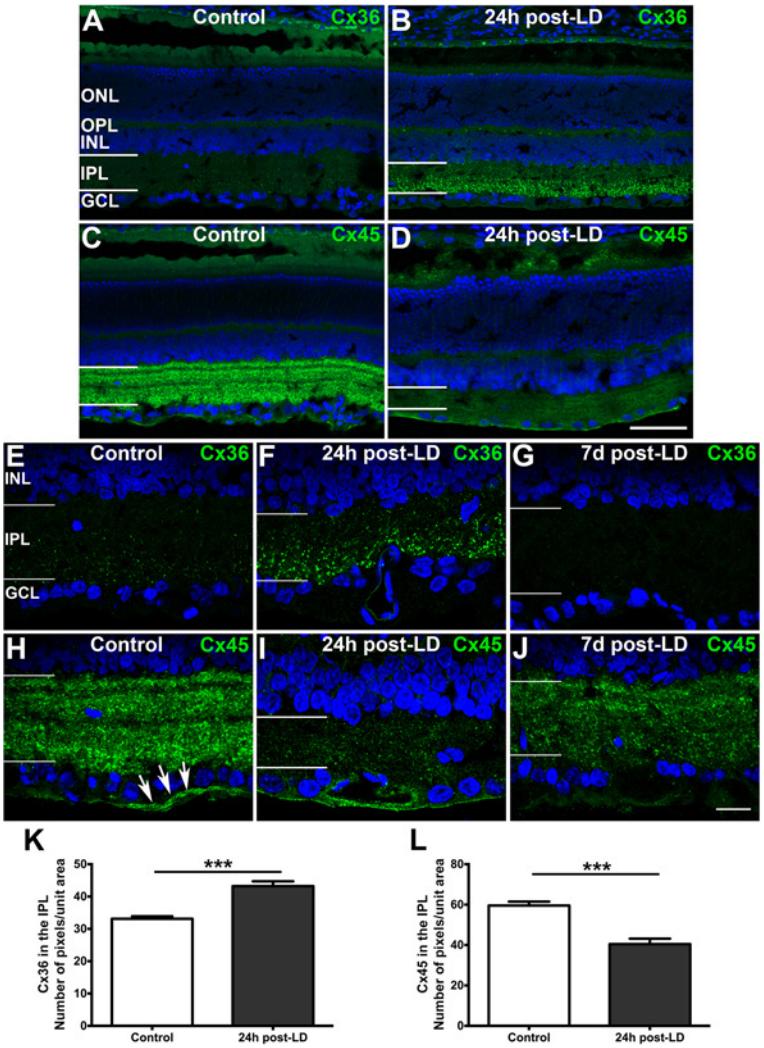

Figure 2. Cx36 and Cx45 expression in control and light-damaged retina. **A**: Cx36 showed little immunoreactivity in the retina of non-light-damaged control animals. **B**: Increased Cx36 expression in the retina collected at 24 h following light damage (LD). **C**: Cx45 immunoreactivity in the control retina. **D**: Decreased Cx45 expression in the retina at 24 h following light damage. **E**–**G**: Cx36 immunoreactivity in the inner retina from the control rat (**E**) and light-damaged rat at 24 h (**F**) and 7 days (**G**) post-LD. The Cx36 immunoreactivity levels are comparable between the control and 7 days post-LD (n = 5; p = 0.6), but were significantly increased at 24 h post-LD (see quantification in K, n = 6, *** p<0.001). **H**–**J**: Cx45 immunoreactivity in the control retina (**H**), and the retina at 24 h (**I**) and 7 days (**J**) post-LD. The expression levels of Cx45 in the inner plexiform layer were similar and statistically insignificant (n = 6, p = 0.1) between the control retina and 7 days post-LD. However, there was a marked decrease in Cx45 in the plexiform layer at the 24 h post injury (**I** and quantification in **L**). The control tissue showed stronger Cx45 labeling in the vascular smooth muscle and possibly astrocytes in the nerve fiber layer (**H**, arrows), which remained constant at 24 h post-LD (**I**), but returned to the level comparable to the control by 7 days post-LD (**J**). All data presented are the mean±standard error of the mean (SEM). Abbreviations: INL, inner nuclear layer; IPL, inner plexiform layer; GCL, ganglion cell layer; LD, light damage. Scale bar = 50 µm in **A**–**D**; scale bar = 20 µm in **E**–**J**.

Quantification indicated a significant decrease in the inner plexiform layer labeling (Figure 2L, Student *t* test, p<0.001). However, by 7 days after the onset of light damage, the expression of Cx45 in the inner plexiform layer had returned with a pattern and level similar to that of the control, but there was now no expression in the nerve fiber layer (Figure 2J).

Expression of connexin 43 increases following light damage: Expression of the gap junction protein Cx43 in the non-light-damaged control group was compared to the light-damaged groups with various recovery periods using western blot. Cx43 was present in the choroid and in the retina before and after light damage (Figure 3). Quantification analysis of the western blots showed that the Cx43 level in the choroid and the

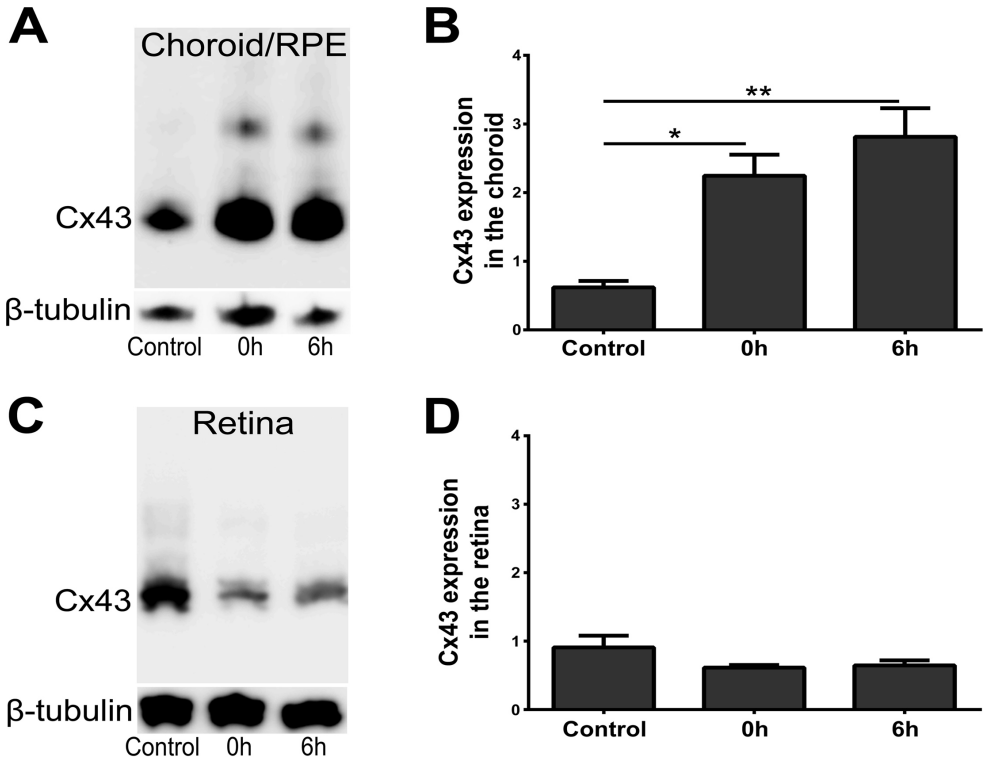

Figure 3. Western blot analysis of Cx43 expression in the choroid and retina of the control and light-damaged animals. **A**: Western blot detection of Cx43 in the control and light-damaged rat choroid and RPE. **B**: Quantitative analysis of western blot for Cx43 protein expression in the choroid and the RPE from the control and light-damaged groups. Cx43 expression was significantly increased 6 h post-exposure compared to the control (n = 6; ** $p<0.01$). There was no statistically significant difference between the control and 0 h groups. **C**: Western blot detection of Cx43 in the control and light-damaged rat retina. **D**: Quantitative analysis of western blot for Cx43 expression in the retina from the control and light-damaged groups. The expression of Cx43 tended to be decreased post-exposure, but this change was not significant (n = 6). Abbreviation: RPE, retinal pigment epithelium.

RPE was significantly increased in the short-term following light damage (Figure 3A,B; one-way ANOVA, $p<0.01$ for 6 h and $p<0.05$ for 0 h). However, the expression level of Cx43 in the retina, although there is a trend of decreased expression, was not statistically significant compared to the control tissue (Figure 3C,D, $p = 0.22$).

Confocal images demonstrated that Cx43 was expressed in the RPE and the choroid (Figure 4A). Following light damage, stronger immunoreactivity of Cx43 was observed mainly in the RPE 0 h post-exposure (Figure 4B) and in the RPE and the choroid 6 h post-exposure (Figure 4C). Cx43 remained high at 24 h (Figure 4D) and 48 h (Figure 4E), but after 7 days appeared to be decreasing again (Figure 4F).

In the normal rat retina, Cx43 immunoreactivity was detected primarily in the ganglion cell layer (Figure 5A), which may be closely associated with the processes of astrocytes and the endothelium of the blood vessels. After light damage and up to 7 days post-exposure, Cx43 immunoreactivity was still detected in the ganglion cell layer and did not seem to be labeled in other cells or layers of the retina (Figure 5B–F).

Connexin 43 expression is detected in macrophages after light damage: Closer analysis of the labeling pattern of Cx43 expression in the choroid using double-labeling immunohistochemistry showed an association between Cx43 and inflammatory cells and oxidative stress markers. In the non-light-damaged choroid, there were CD45 immunolabeled macrophages, but they did not colocalize with Cx43 (Figure 6A–C). Cx43 was not only increased in amount but also coexpressed on some CD45 immunolabeled macrophages 24 h after light damage (Figure 6D-F). Interestingly, expression of Cx43 was also detected on nitrotyrosine immunolabeled cells in the choroid post-exposure (Figure 7D-F), a feature not seen in the non-light-damaged control (Figure 7A-C).

We further analyzed nitrotyrosine-labeled cells in the light-damaged choroid by investigating the expression of the ionized calcium-binding adaptor molecule-1 (Iba-1). Iba-1 recognizes all dendritic-derived macrophages and has been proven to be a reliable marker for microglia in the nervous system [33]. Colocalization of nitrotyrosine and Iba-1 demonstrated that the nitrotyrosine-labeled cells are Iba-1-positive macrophages seen at 6 h and at 24 h after light damage (Figure 8).

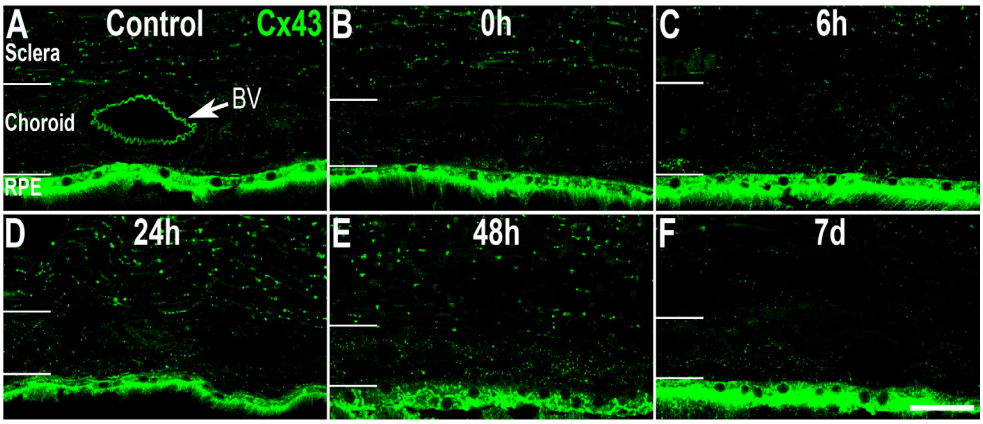

Figure 4. Cx43 immunoreactivity in the control and light-damaged retinal pigment epithelium and choroid. **A**: Cx43 immunoreactivity in non-light-damaged control RPE/choroid tissue. Cx43 immunolabeling was seen in the choroid, the sclera and strongly in the RPE. **B**–**F**: Increased Cx43 immunoreactivity was seen in the RPE and choroid tissue from the light-damaged group at the various recovery time points. Autofluorescence form elastic lamina surrounding a blood vessel is seen in **A** (arrow). Abbreviations: RPE, retinal pigment epithelium; LD, light damage; BV, blood vessel. Scale bar = 50 µm.

DISCUSSION

In the present study, we have documented that 24 h intense light exposure results in changes in the expression of connexin proteins in the light-damaged albino rat eye. Immunohistochemical analysis showed that Cx36 was significantly increased in the inner plexiform layer, and Cx45 was significantly decreased in the same region 24 h after intense light exposure. The changes in the expression of Cx43 were particularly interesting. Within a short period after light exposure, the Cx43 protein level was significantly increased in the choroid, but not in the retina. Further investigation showed that increased Cx43 expression was colocalized with an oxidative stress marker, nitrotyrosine, and with CD45-positive macrophages, suggesting Cx43 has a close association with the inflammatory process in this tissue.

Alterations in connexin 36 and connexin 45 expression levels may contribute to light adaptation in the light-damaged animal model: Previous studies on the rat retina have demonstrated that Cx36 is expressed on AII amacrine cells, ON cone bipolar cells, and alpha retinal ganglion cells that are the key elements of the light signal transduction pathways [7]. The current study showed that Cx36 is increased in the inner region of the retinal inner plexiform layer within 24 h following light damage. This finding is consistent with previous reports on Cx36 expression levels in dark- or light-exposed animals [34-36]. Although we found increased expression of Cx36 in the light-damaged retina, the transcript

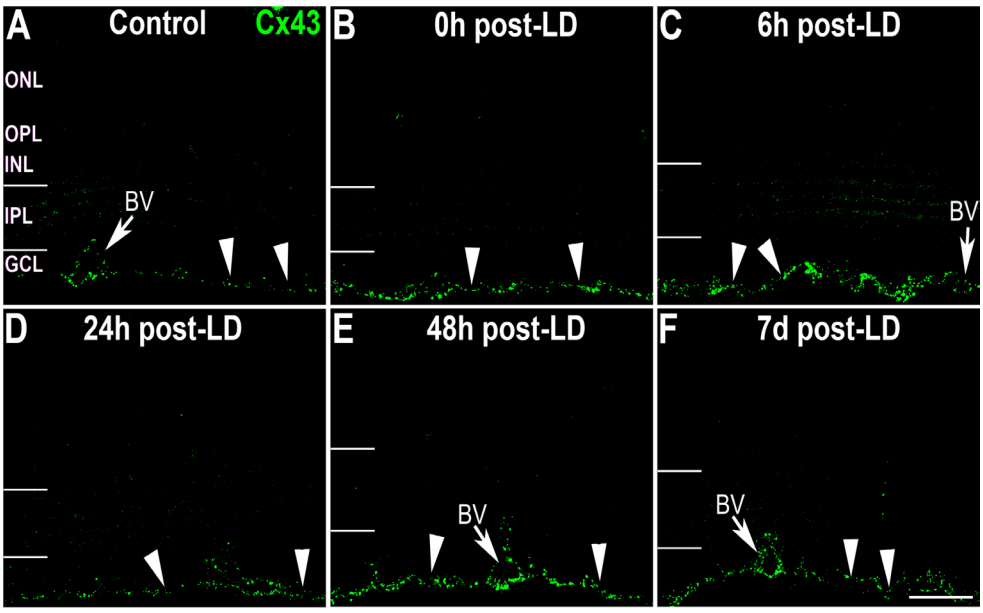

Figure 5. Confocal images showing Cx43 expression in the control and light-damaged retina. **A**: Cx43 immunoreactivity was limited to the ganglion cell layer in the normal control retina. **B**–**F**: Cx43 immunolabeling in the retina at various recovery time points following light damage; there was no apparent change in the expression levels. Abbreviations: ONL, outer nuclear layer; OPL, outer plexiform layer; INL, inner nuclear layer; IPL, inner plexiform layer; GCL, ganglion cell layer; BV, blood vessels; LD, light damage. Scale bar = 50 µm.

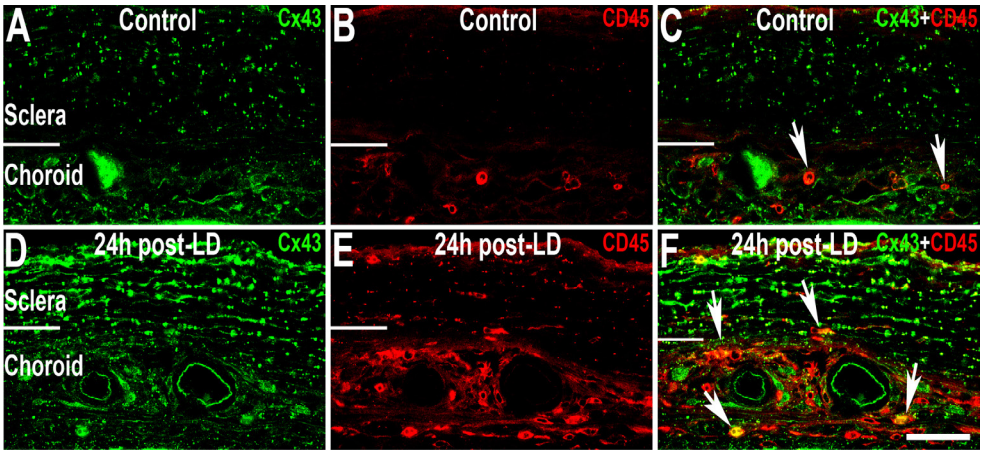

Figure 6. Colocalization of Cx43 and CD45 was seen only in the light-damaged choroid. **A**–**C**: Cx43 labeling (**A**), CD45 labeling (**B**), and combined images (**C**) in the non-light-damaged choroid. CD45 immunolabeled macrophages did not show Cx43 coexpression. **D**–**F**: Cx43 labeling (**D**), CD45 labeling (**E**), and combined images (**F**) at 24 h post-LD. Many CD45 immunolabeled macrophages (arrows in **F**) showed Cx43 immunoreactivity in the choroid at this time point. Abbreviations: LD, light damage. Scale bar = 50 µm.

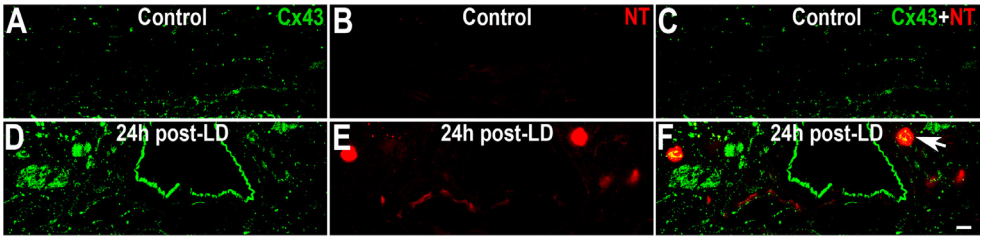

Figure 7. Colocalization of Cx43 and nitrotyrosine was seen only in the light-damaged choroid. **A**–**C**: Cx43 labeling (**A**), nitrotyrosine labeling (**B**), and combined images (**C**) in the non-light-damaged choroid. Immunoreactivity to nitrotyrosine, an oxidative stress marker, was barely detectable. **D**–**F**: Cx43 labeling (**D**), nitrotyrosine (**E**), and combined images (**F**) in the light-damaged choroid at 24 h post-LD. Nitrotyrosine immune-labeled cells showed coexpression of Cx43 (arrow in **F**) in the choroid. Abbreviations: NT, nitrotyrosine; LD, light damage. Scale bar = 10 µm.

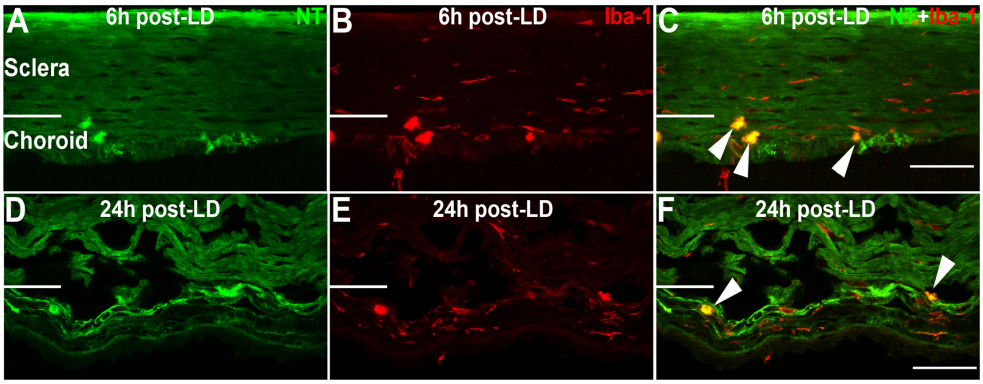

Figure 8. Nitrotyrosine-labeled cells were ionized calcium-binding adaptor molecule-1-positive macrophages in light-damaged choroid. **A**–**C**: Immunolabeling for nitrotyrosine (**A**), ionized calcium-binding adaptor molecule-1 (Iba-1) (**B**), and combined images (**C**), seen here at 6 h post-injury. **D**–**F**: Immunolabeling for nitrotyrosine (**D**), Iba-1 (**E**), and combined images (**F**), seen here at 24 h post-injury. Nitrotyrosine was colocalized with Iba-1 expression on macrophages (arrow heads in **C** and **F**). Abbreviations: NT, nitrotyrosine; LD, light damage. Scale bar = 50 µm.

and protein levels of Cx36 were significantly decreased after dark-adaptation in the mouse retina [36]. Increased Cx36 protein in the inner plexiform layer has been demonstrated to be associated with secondary cell loss in laser-created retinal lesions, and Cx36-deficient ($Cx36^{-/-}$) mice exhibit a significant increase in cell death after trauma [35]. These data must be interpreted with some caution since, as noted, Cx45 and Cx36 are known to change expression with light-dark adaptation. In this study, returning animals to normal light after intense light for 24 h could either appear as a light reduction (dark adaptation), or their circadian rhythms may have been disrupted. Some of the change in these connexins might then simply reflect disruption of light-dark adaptation pathways.

In addition to Cx36, our results for the immunohistochemical labeling showed a significant decrease in Cx45 immunoreactivity in the light-damaged retina compared to the control tissue. Cx45 is expressed on AII amacrine cells, ON cone bipolar cells, and alpha retinal ganglion cells in the rat retina [7]. Interestingly, another study reported that these cells participate in enhanced electrical coupling between alpha ganglion cells in the albino rabbit retina from night to day [34]. To the best of our knowledge, changes in Cx45 expression in the light-damaged animal have not been reported. Findings of connexin protein levels in the mouse retina following prolonged dark-exposure are not parallel with our results but have shown that the transcript of Cx45 is significantly decreased in response to dark-adaptation [36].

Heterotypic electrical synapses are formed between Cx36 located in AII amacrine cells and Cx45 located in ON cone bipolar cells in the inner plexiform layer, and $Cx36^{-/-}$ mice and $Cx45^{-/-}$ mice show decreased activity of the retinal interneurons in the rod and cone pathways [37]. The current study has demonstrated that the changes in Cx36 and Cx45 are restricted to the inner plexiform layer in the light-damaged retina, where bipolar cells, amacrine cells, and ganglion cells interact. This indicates that in addition to the RPE and photoreceptors in the outer retina, intense light exposure also leads to neuron reactions in the inner retina. The Cx36 and Cx45 expression changes suggest that these two connexin proteins react to photoreceptor damage and provide further evidence that Cx36 is associated with Cx45 in intercellular communications between inner retinal neurons in the light transduction pathway.

Increased connexin 43 expression is primarily in the choroid and the RPE in the light-damaged animal model: This study has demonstrated that Cx43 protein expression is significantly increased in the choroid and the RPE following light damage but little change was detected in the retina itself, which may be because the whole retina was used for western blotting analysis instead of selective use of the dorsal retina, which was the most stressed/damaged area. Cx43 upregulation in the light-damaged choroid and RPE is parallel with many studies on animal models of central nervous system (CNS) injuries [38,39]. Increased Cx43 protein and transcript have also been found in many human CNS injuries and diseases, including stroke, epilepsy, and Huntington's disease [16-18]. The immunoreactivity of Cx43 is upregulated in the human glaucomatous retina compared to normal retinal tissue [15]. Increased Cx43 expression is mainly seen in the astrocytes located in the retinal ganglion cell layer of the peripapillary and mid-peripheral regions. In the peripapillary region, upregulated Cx43 is also expressed along glial fibrillary acidic protein (GFAP)-labeled Müller cell processes throughout the entire retina. Retinal endothelial cells retain the same expression level of Cx43 in the glaucomatous retina as the controls [15]. Elevated Cx43 expression was also detected in the rat retina, parallel with changes in GFAP immunoreactivity and ganglion cell loss following optic nerve injury [40]. It is interesting, therefore, to compare the changes seen in Cx43 following light damage in the albino rat model where it appeared to be restricted primarily to the choroid and the RPE.

Changes in connexin 43 expression is associated with oxidative stress and inflammation in light-damaged tissue: The present study found that the upregulated expression of Cx43 was throughout the choroid but notably colocalized with CD45-positive macrophages in the choroid and the retina following light damage. A previous in vitro study showed that upregulated Cx43 protein was detected in the primary culture of microglia after treatment with bacterial lipopolysaccharide (LPS) plus interferon-γ (INF-γ) or tumor necrosis factor-α (TNF-α) plus INF-γ [41]. Monocytes and macrophages express Cx43 only after being stimulated by exposure to IFN-γ and TNF-α but not under physiologic conditions [42]. Hemichannels constituted of Cx43 are located in the astrocytes of the CNS, and electrophysiological studies have indicated that these hemichannels are likely to be closed under physiologic conditions and to be opened under pathological conditions, such as oxidative stress [43]. A more recent study demonstrated that expression of Cx43 by activated phagocytes is critical for regulating phagocytosis and rearranging the F-actin cytoskeleton [44]. Cx43 is also expressed on many other residential and circulating leukocytes, including neutrophils, dendritic cells, and lymphocytes [45]. However, thus far, relatively little has been reported on Cx43 expression by inflammatory cells in tissue from in vivo investigations. Results from the present study suggest that Cx43 is expressed on activated macrophages in the choroid following intense light exposure, which may be critical for the role of

these inflammatory cells. Many studies have suggested the involvement of the complement system in the choroid that may contribute to late AMD [23,46]. Results from this study using the light-damaged animal model indicate that Cx43 expression in macrophages may also be an important factor in pathogenesis and disease progression of early AMD. Tuning down the function of Cx43 may result in downregulation of the inflammatory response in the tissue as is seen after downregulation of Cx43 in skin wounds [47,48], liver failure [49], arthritis [50], and spinal cord injury [39,51].

The present study has shown that the expression of Cx43 was also detected in the nitrotyrosine-labeled macrophages in the choroid following light damage. Nitrotyrosine as a marker of protein nitration is increased in the photoreceptor outer segment and the RPE in the light-damaged animal model, when compared to the animals maintained in the dark [52]. Colocalization of nitrotyrosine and Iba-1 in the light-damaged choroid indicates a close association between oxidative stress and inflammatory responses. The lipid whisker model suggests that oxidized phospholipids from senescent and apoptotic cells can be recognized by receptors on macrophages and are then cleared up by the innate immune system [53]. In this study, nitrotyrosine immunoreactivity detected in the Iba-1 immunolabeled cells has provided a good indication of where the oxidized phospholipids end up. These findings suggest that oxidative stress is a preamble for the inflammatory responses that follow.

In summary, the present study has revealed changes in Cx36 and Cx45 expression in the retina in the light-damaged albino rat model. Increased Cx43 expression has been detected in the choroid following light damage, and this increase is closely associated with tissue damage, including oxidative stress and inflammation. Findings from the present study contribute to better understanding of tissue dysfunction and injury process occurring in the light-damaged albino rat model. This study also suggests that gap junction channels, particularly Cx43 channels, may be potential sites that contribute to reduced visual loss in some ocular diseases and injuries.

ACKNOWLEDGMENTS

Grant information: This work was supported in part by the Health Research Council of New Zealand, reference number: 09/157; 2) Auckland Medical Research Foundation, reference number: 1109007; 3) Faculty Research Development Fund, reference number: 3624490.

REFERENCES

1. Yeager M. Structure of cardiac gap junction intercellular channels. J Struct Biol 1998; 121:231-45. [PMID: 9615440].
2. Kumar NM, Gilula NB. The gap junction communication channel. Cell 1996; 84:381-8. [PMID: 8608591].
3. Goodenough DA, Goliger JA, Paul DL. Connexins, connexons, and intercellular communication. Annu Rev Biochem 1996; 65:475-502. [PMID: 8811187].
4. Goodenough DA, Paul DL. Beyond the gap: functions of unpaired connexon channels. Nat Rev Mol Cell Biol 2003; 4:285-94. [PMID: 12671651].
5. Evans WH, De Vuyst E, Leybaert L. The gap junction cellular internet: connexin hemichannels enter the signalling limelight. Biochem J 2006; 397:1-14. [PMID: 16761954].
6. Spray DC, Ye ZC, Ransom BR. Functional connexin "hemichannels": a critical appraisal. Glia 2006; 54:758-73. [PMID: 17006904].
7. Bloomfield SA, Volgyi B. The diverse functional roles and regulation of neuronal gap junctions in the retina. Nat Rev Neurosci 2009; 10:495-506. [PMID: 19491906].
8. Söhl G, Güldenagel M, Traub O, Willecke K. Connexin expression in the retina. Brain Res Brain Res Rev 2000; 32:138-45. [PMID: 10751663].
9. Kerr NM, Johnson CS, de Souza CF, Chee KS, Good WR, Green CR, Danesh-Meyer HV. Immunolocalization of gap junction protein connexin43 (GJA1) in the human retina and optic nerve. Invest Ophthalmol Vis Sci 2010; 51:4028-34. [PMID: 20375327].
10. Perez Velazquez JL, Frantseva MV, Naus CC. Gap junctions and neuronal injury: protectants or executioners? Neuroscientist 2003; 9:5-9. [PMID: 12580335].
11. Goodenough DA, Paul DL. Gap junctions. Cold Spring Harb Perspect Biol 2009; 1:a002576-[PMID: 20066080].
12. Ripps H. Cell death in retinitis pigmentosa: gap junctions and the 'bystander'effect. Exp Eye Res 2002; 74:327-36. [PMID: 12014914].
13. Davidson JO, Green CR. B Nicholson LF, O'Carroll SJ, Fraser M, Bennet L, Jan Gunn A. Connexin hemichannel blockade improves outcomes in a model of fetal ischemia. Ann Neurol 2012; 71:121-32. [PMID: 22275258].
14. Ly A, Yee P, Vessey KA, Phipps JA, Jobling AI, Fletcher EL. Early inner retinal astrocyte dysfunction during diabetes and development of hypoxia, retinal stress, and neuronal functional loss. Invest Ophthalmol Vis Sci 2011; 52:9316-26. [PMID: 22110070].
15. Kerr NM, Johnson CS, Green CR, Danesh-Meyer HV. Gap junction protein connexin43 (GJA1) in the human glaucomatous optic nerve head and retina. J Clin Neurosci 2011; 18:102-8. [PMID: 20934339].
16. Elisevich K, Rempel SA, Smith BJ, Edvardsen K. Hippocampal connexin 43 expression in human complex partial seizure disorder. Exp Neurol 1997; 145:154-64. [PMID: 9184118].

17. Nakase T, Yoshida Y, Nagata K. Enhanced connexin 43 immunoreactivity in penumbral areas in the human brain following ischemia. Glia 2006; 54:369-75. [PMID: 16886200].

18. Vis JC, Nicholson L, Faull R, Evans W, Severs N, Green C. Connexin expression in Huntington's diseased human brain. Cell Biol Int 1998; 22:837-47. [PMID: 10873295].

19. Noell WK, Walker VS, Kang BS, Berman S. Retinal damage by light in rats. Invest Ophthalmol 1966; 5:450-73. [PMID: 5929286].

20. Marc RE, Jones BW, Watt CB, Vazquez-Chona F, Vaughan DK, Organisciak DT. Extreme retinal remodeling triggered by light damage: implications for age related macular degeneration. Mol Vis 2008; 14:782-806. [PMID: 18483561].

21. Wu T, Handa JT, Gottsch JD. Light-induced oxidative stress in choroidal endothelial cells in mice. Invest Ophthalmol Vis Sci 2005; 46:1117-23. [PMID: 15790868].

22. Khandhadia S, Lotery A. Oxidation and age-related macular degeneration: insights from molecular biology. Expert Rev Mol Med 2010; 12:e34-[PMID: 20959033].

23. Anderson DH, Mullins RF, Hageman GS, Johnson LV. A role for local inflammation in the formation of drusen in the aging eye. Am J Ophthalmol 2002; 134:411-31. [PMID: 12208254].

24. Khandhadia S, Cipriani V, Yates J, Lotery AJ. Age-related macular degeneration and the complement system. Immunobiology 2012; 217:127-46. [PMID: 21868123].

25. Rutar M, Provis JM, Valter K. Brief exposure to damaging light causes focal recruitment of macrophages, and long-term destabilization of photoreceptors in the albino rat retina. Curr Eye Res 2010; 35:631-43. [PMID: 20597649].

26. Zhang C, Shen JK, Lam TT, Zeng HY, Chiang SK, Yang F, Tso MOM. Activation of microglia and chemokines in light-induced retinal degeneration. Mol Vis 2005; 11:887-95. [PMID: 16270028].

27. Coorey NJ, Shen W, Chung SH, Zhu L, Gillies MC. The role of glia in retinal vascular disease. Clin Exp Optom 2012; 95:266-81. [PMID: 22519424].

28. Yu TY, Acosta ML, Ready S, Cheong YL, Kalloniatis M. Light exposure causes functional changes in the retina: increased photoreceptor cation channel permeability, photoreceptor apoptosis, and altered retinal metabolic function. J Neurochem 2007; 103:714-24. [PMID: 17623037].

29. Hollyfield JG, Bonilha VL, Rayborn ME, Yang XP, Shadrach KG, Lu L, Ufret RL, Salomon RG, Perez VL. Oxidative damage-induced inflammation initiates age-related macular degeneration. Nat Med 2008; 14:194-8. [PMID: 18223656].

30. Danesh-Meyer HV, Kerr NM, Zhang J, Eady EK, O'Carroll SJ, Nicholson LFB, Johnson CS, Green CR. Connexin43 mimetic peptide reduces vascular leak and retinal ganglion cell death following retinal ischaemia. Brain 2012; 135:506-20. [PMID: 22345088].

31. Organisciak DT, Vaughan DK. Retinal light damage: mechanisms and protection. Prog Retin Eye Res 2010; 29:113-34. [PMID: 19951742].

32. Acosta ML, Kalloniatis M, Christie DL. Creatine transporter localization in developing and adult retina: importance of creatine to retinal function. Am J Physiol Cell Physiol 2005; 289:C1015-23. [PMID: 15930147].

33. Ahmed Z, Shaw G, Sharma VP, Yang C, McGowan E, Dickson DW. Actin-binding proteins coronin-1a and IBA-1 are effective microglial markers for immunohistochemistry. J Histochem Cytochem 2007; 55:687-700. [PMID: 17341475].

34. Hu EH, Pan F, Völgyi B, Bloomfield SA. Light increases the gap junctional coupling of retinal ganglion cells. J Physiol 2010; 588:4145-63. [PMID: 20819943].

35. Striedinger K, Petrasch, Parwez E, Zoidl G, Napirei M, Meier C, Eysel UT, Dermietzel R. Loss of connexin36 increases retinal cell vulnerability to secondary cell loss. Eur J Neurosci 2005; 22:605-16. [PMID: 16101742].

36. Kihara AH, Mantovani de Castro L, Moriscot AS, Hamassaki DE. Prolonged dark adaptation changes connexin expression in the mouse retina. J Neurosci Res 2006; 83:1331-41. [PMID: 16496335].

37. Söhl G, Maxeiner S, Willecke K. Expression and functions of neuronal gap junctions. Nat Rev Neurosci 2005; 6:191-200. [PMID: 15738956].

38. Haupt C, Witte O, Frahm C. Temporal profile of connexin 43 expression after photothrombotic lesion in rat brain. Neuroscience 2007; 144:562-70. [PMID: 17112677].

39. O'Carroll SJ, Alkadhi M, Nicholson LF, Green CR. Connexin 43 mimetic peptides reduce swelling, astrogliosis, and neuronal cell death after spinal cord injury. Cell Commun Adhes 2008; 15:27-42. [PMID: 18649176].

40. Chew SSL, Johnson CS, Green CR, Danesh-Meyer HV. Response of retinal Connexin43 to optic nerve injury. Invest Ophthalmol Vis Sci 2011; 52:3620-9. [PMID: 21310901].

41. Eugenín EA, Eckardt D, Theis M, Willecke K, Bennett MVL, Sáez JC. Microglia at brain stab wounds express connexin 43 and in vitro form functional gap junctions after treatment with interferon-γ and tumor necrosis factor-α. Proc Natl Acad Sci USA 2001; 98:4190-5. [PMID: 11259646].

42. Eugenín EA, Brañes MC, Berman JW, Sáez JC. TNF-α plus IFN-γ induce connexin43 expression and formation of gap junctions between human monocytes/macrophages that enhance physiological responses. J Immunol 2003; 170:1320-8. [PMID: 12538692].

43. Sáez JC, Contreras JE, Bukauskas FF, Retamal MA, Bennett MV. Gap junction hemichannels in astrocytes of the CNS. Acta Physiol Scand 2003; 179:9-22. [PMID: 12940934].

44. Anand RJ, Dai S, Gribar SC, Richardson W, Kohler JW, Hoffman RA, Branca MF, Li J, Shi X-H, Sodhi CP. A role for connexin43 in macrophage phagocytosis and host survival after bacterial peritoneal infection. J Immunol 2008; 181:8534-43. [PMID: 19050272].

45. Pfenniger A, Chanson M, Kwak BR. Connexins in atherosclerosis. Biochimica et Biophysica Acta (BBA)- Biomembranes 2013; 1828:157-66. .

46. Ambati J, Anand A, Fernandez S, Sakurai E, Lynn BC, Kuziel WA, Rollins BJ, Ambati BK. An animal model of age-related macular degeneration in senescent Ccl-2- or Ccr-2-deficient mice. Nat Med 2003; 9:1390-7. [PMID: 14566334].

47. Mori R, Power KT, Wang CM, Martin P, Becker DL. Acute downregulation of connexin43 at wound sites leads to a reduced inflammatory response, enhanced keratinocyte proliferation and wound fibroblast migration. J Cell Sci 2006; 119:5193-203. [PMID: 17158921].

48. Qiu C, Coutinho P, Frank S, Franke S, Law LY, Martin P, Green CR, Becker DL. Targeting connexin43 expression accelerates the rate of wound repair. Curr Biol 2003; 13:1697-703. [PMID: 14521835].

49. Balasubramaniyan V, Dhar DK, Warner AE, Li W-YV, Amiri AF, Bright B, Mookerjee RP, Davies NA, Becker DL, Jalan R. Importance of Connexin-43 based gap junction in cirrhosis and acute on chronic liver failure. J Hepatol 2013; 85:1194-1200. [PMID: 23376361].

50. Tsuchida S, Arai Y, Kishida T, Takahashi KA, Honjo K, Terauchi R, Inoue H, Oda R, Mazda O, Kubo T. Silencing the expression of connexin 43 decreases inflammation and joint destruction in experimental arthritis. J Orthop Res 2013; 31:525-530. [PMID: 23165424].

51. Cronin M, Anderson PN, Cook JE, Green CR, Becker DL. Blocking connexin43 expression reduces inflammation and improves functional recovery after spinal cord injury. Mol Cell Neurosci 2008; 39:152-60. [PMID: 18617007].

52. Palamalai V, Darrow RM, Organisciak DT, Miyagi M. Light-induced changes in protein nitration in photoreceptor rod outer segments. Mol Vis 2006; 12:1543-51. [PMID: 17200653].

53. Greenberg ME, Li XM, Gugiu BG, Gu X, Qin J, Salomon RG, Hazen SL. The lipid whisker model of the structure of oxidized cell membranes. J Biol Chem 2008; 283:2385-96. [PMID: 18045864].

54. Rash JE, Yasumura T, Dudek FE, Nagy JI. Cell-specific expression of connexins and evidence of restricted gap junctional coupling between glial cells and between neurons. J Neurosci 2001; 21:1983-2000. [PMID: 11245683].

55. Li X, Kamasawa N, Ciolofan C, Olson CO, Lu S, Davidson KGV, Yasumura T, Shigemoto R, Rash JE, Nagy JI. Connexin45-containing neuronal gap junctions in rodent retina also contain connexin36 in both apposing hemiplaques, forming bihomotypic gap junctions, with scaffolding contributed by zonula occludens-1. J Neurosci 2008; 28:9769-89. [PMID: 18815262].

56. Ishida S, Ishida S, Yamashiro K, Usui T, Kaji Y, Ogura Y, Hida T, Honda Y, Oguchi Y. Leukocytes mediate retinal vascular remodeling during development and vaso-obliteration in disease. Nat Med 2003; 9:781-8. [PMID: 12730690].

57. Robertson MJ, Robertson MJ, Erwig LP, Liversidge J, Forrester JV, Rees AJ. Retinal microenvironment controls resident and infiltrating macrophage function during uveoretinitis. Invest Ophthalmol Vis Sci 2002; 43:2250-7. [PMID: 12091424].

58. Du Y, Du YP, Smith MA, Miller CM. Diabetes-induced nitrative stress in the retina, and correction by aminoguanidine. J Neurochem 2002; 80:771-9. [PMID: 11948240].

59. Xu H, Chen M, Manivannan A, Lois N, Forrester JV. Age-dependent accumulation of lipofuscin in perivascular and subretinal microglia in experimental mice. Aging Cell 2008; 7:58-68. [PMID: 17988243].

60. Sappington RM, Calkins DJ. Contribution of TRPV1 to microglia-derived IL-6 and NFkappaB translocation with elevated hydrostatic pressure. Invest Ophthalmol Vis Sci 2008; 49:3004-17. [PMID: 18362111].

Articles are provided courtesy of Emory University and the Zhongshan Ophthalmic Center, Sun Yat-sen University, P.R. China. The print version of this article was created on 27 May 2014. This reflects all typographical corrections and errata to the article through that date. Details of any changes may be found in the online version of the article.